DOI: 10.53469/jpce.2025.07(02).07

Energy Method for Deformation Analysis of Flexible Pile Composite Foundation Under Lateral Restriction

Chuang Nie[1], Jie Liu[2]

[1,2]School of Civil Engineering, Hunan University of Technology, Zhuzhou 412007, China
[1]cnie0808@163.com, [2]2280017034@qq.com

Abstract: ***To limit the lateral extrusion and compression deformation of soft soil within the load-bearing range, and effectively control the settlement of soft soil foundations, a new technology for side-limited flexible pile composite foundation and energy method for deformation analysis has been proposed. Based on certain assumptions, the compo-site reinforcement area within the side limit and the natural foundation within the de-formation influence depth are considered as a whole, and the displacement component expressions that satisfy the displacement boundary conditions are constructed, leading to the formulation of the total potential energy equation for the system. Based on the principle of potential energy extremum, a displacement variational equation for the system is established, and an approximate analytical algorithm for deformation analysis of flexible pile composite foundation under side limit conditions is proposed. The rationality of the theoretical analysis method is verified by FLAC3D numerical simulation results and on-site monitoring results.***

Keywords: Subgrade Engineering, Flexible Pile Composite Foundation, Energy Method, Load-Settlement Relation, Displacement Variational Equation.

1. Introduction

Saturated soft clays such as mud and muddy soils are widely distributed in the coastal areas of our country. These soft soils are characterized by high water content, large compressibility, and significant lateral extrusion. The lateral extrusion of soft soil not only affects the magnitude of settlement but, more importantly, influences the forces on adjacent buildings and structures. Excessive lateral deformation can also affect the stability of the foundation. Currently, research on the deformation of soft foundations under embankments mainly focuses on settlement calculation and prediction, with less attention given to lateral displacement studies. The settlement calculation of embankments usually adopts the one-dimensional settlement calculation method specified by standards. The one-dimensional settlement calculation method assumes that the soil is elastic, the stress distribution conforms to the Boussinesq solution, there is no lateral deformation, and only vertical compression occurs.

Previous research results indicate that when the thickness of the compressible soil layer is much smaller compared to the area of the base load distribution, this assumption basically holds true [1-2]. For soft soil foundations, the horizontal extrusion of soft soil causes an increase in the total settlement of the foundation, and the lateral deformation of the soil has a very significant impact on settlement. The lateral displacement varies with the horizontal distance from the point of analysis to the centerline, and is generally larger under the shoulder points of the embankment [3]. The magnitude of lateral displacement is related to the properties of the soft soil, its position, and the height of the embankment. The softer the soil, the thicker the soft soil, the shallower the burial depth, and the higher the embankment, the greater the lateral deformation, and the corresponding settlement will be larger. In this case, the settlement calculation results that do not consider the influence of lateral deformation are underestimated [3]. Research on the impact of lateral soil displacement on foundation settlement has been ongoing. Tu and others [4-9] used the finite element method to study the influence of soil lateral expansion on the settlement of embankments. Ye and others [10-16] systematically analyzed the impact of lateral soil displacement on the settlement of roadbeds, and pointed out that restricting the lateral displacement of the section under the slope angle of the embankment is the most effective measure to reduce embankment settlement [17-27]. Based on the results of vertical consolidation comparison tests under different lateral constraint conditions, the influence of lateral constraints on the settlement characteristics and deformation parameters of soft clay was analyzed, and relevant numerical simulation studies were also conducted.

To restrict the lateral extrusion and compressive deformation of soft soil within the load-bearing area, reduce foundation settlement, and mitigate the adverse impact of additional loads on the surrounding environment, our research team proposes the installation of one or multiple rows of soil-cement mixing piles outside the load-bearing area to form block or grid-shaped soil-cement walls that limit the lateral deformation of soft soil. Within the load-bearing area, a soil-cement mixing pile composite foundation is used to reduce the compressive deformation of soft soil (as shown in Figure 1), thereby effectively reducing the settlement of the composite foundation. On the basis of certain assumptions, the pile-soil composite reinforcement area within the lateral restriction range and the natural foundation within the deformation influence depth range are considered as a whole. A displacement component expression that satisfies the displacement boundary conditions has been constructed, and an approximate analytical algorithm for the deformation analysis of composite foundations under lateral restriction conditions has been proposed. Through examples, the FLAC3D numerical simulation results, theoretical analysis results, and field monitoring results have been compared, validating the rationality of the theoretical analysis method.

2. Computational Model and Displacement Variational Method

2.1 Basic Assumptions and Computational Model

This paper focuses on the soft foundation of highways as the subject of study, with the embankment load being equivalently modeled as a trapezoidal distributed load.

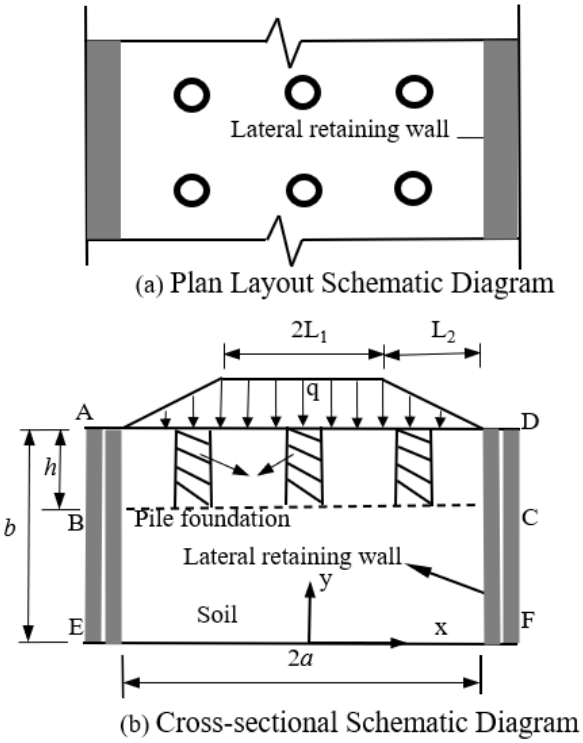

Figure 1: Model of analysis on composite foundation

Highways are linear structures that can be considered infinitely long in the longitudinal direction. Taking any cross-section as the plane composed of the x-axis and y-axis, with the direction of the travel lane as the z-axis, under the action of the embankment load, each point in the foundation will only displace along the x and y directions and will not displace in the z direction. Therefore, this problem can be regarded as a plane strain problem.

Assuming that the materials are homogeneous, isotropic, and ideal elastic bodies [28], and neglecting the self-weight of the materials.

The embankment load is applied as an equivalent trapezoidal distributed load directly acting on the top surface of the reinforcement zone (as shown in Figure 1), without considering the influence of the cushion layer. The load acting on the reinforcement zone is:

$$Q = \begin{cases} -q & (-L_1 \le x \le L_1) \\ \frac{-q(L_2+L_1-x)}{L_2} & (L_1 \le x \le L_1+L_2) \end{cases} \quad (1)$$

It is assumed that the horizontal and vertical displacements at the AE and DF interfaces between the lateral soil-cement wall and the soil are linearly related to the y-axis. The horizontal and vertical displacements at the EF boundary are both zero.

The normal forces on the AE and DF interfaces lie between the at-rest earth pressure and the passive earth pressure. For ease of calculation, the passive earth pressure is reduced. The expression is:

$$e_p = k[\gamma(b-y)k_p + 2c\sqrt{k_p}) \quad (2)$$

In the formula: (k) is the reduction coefficient for passive earth pressure, which is a parameter related to the deformation of the lateral soil-cement wall. $k_p = tg^2(45 + \frac{\varphi}{2})$; γ、φ and c represent the unit weight, internal friction angle, and cohesion of the soil outside the reinforcement area, respectively.

For the convenience of analysis, the piles and the soil surrounding the piles in the reinforcement area are equivalently treated as isotropic elastic bodies. The equivalent composite modulus is determined by the area weighting method according to the "Highway Subgrade Design Specifications" (JTJGD30-2004) [7]:

$$E_1 = mE_p + (1-m)E_s \quad (3)$$

In the formula: E_p and E_s represent the elastic moduli of the pile body and the soil between piles, respectively; m represents the replacement ratio of the pile.

2.2 Displacement Variational Method

2.2.1 The displacement boundary conditions of the problem.

Based on the assumptions described earlier, the displacement boundary conditions of the problem are:

$$\left.\begin{array}{l} u(x,y)|_{x=\pm a} = A_1\frac{y}{b}, v(x,y)|_{x=\pm a} = B_1\frac{y}{b} \\ u(x,y)|_{y=0} = 0, v(x,y)|_{y=0} = 0 \end{array}\right\} \quad (4)$$

In the formula, $u(x,y)$ represents the displacement in the x-direction; $v(x,y)$ represents the displacement in the y-direction.

Due to the symmetry of Figure 1, it can be known that: $u(x,y)$ is an odd function of x, and $v(x,y)$ is an even function of x.

2.2.2 Displacement component and total potential energy of the system.

Based on the boundary conditions, symmetry, and anti-symmetry of the problem, the following displacement component expressions are constructed:

$$\left.\begin{array}{l} u(x,y) = A_1\frac{y}{b} + A_2(\frac{x}{a} - \frac{x^3}{a^3})\frac{y}{b} + A_3(\frac{x}{a} - \frac{x^3}{a^3})\frac{y^2}{b^2} \\ v(x,y) = B_1\frac{y}{b} + B_2(1 - \frac{x^2}{a^2})\frac{y}{b} + B_3(1 - \frac{x^2}{a^2})\frac{y^2}{b^2} \end{array}\right\} \quad (5)$$

By comparing Equation (4) with Equation (5), it can be concluded that the pre-scribed displacement components satisfy all the displacement boundary conditions as well as the conditions of symmetry and anti-symmetry.

Using the theory of elasticity, the deformation potential energy of the reinforcement area and the deformation influence area can be obtained respectively:

$$U_1 = \alpha_1 \iint_{ABCD} [(\frac{\partial u}{\partial x})^2 + (\frac{\partial v}{\partial y})^2 + \beta_1 \frac{\partial u}{\partial x}\frac{\partial v}{\partial y} + \gamma_1 (\frac{\partial v}{\partial x} + \frac{\partial u}{\partial y})^2] dxdy \quad (6)$$

$$U_2 = \alpha_2 \iint_{BGHC} [(\frac{\partial u}{\partial x})^2 + (\frac{\partial v}{\partial y})^2 + \beta_2 \frac{\partial u}{\partial x}\frac{\partial v}{\partial y} + \gamma_2 (\frac{\partial v}{\partial x} + \frac{\partial u}{\partial y})^2] dxdy \quad (7)$$

In the formula, U_1 and U_2 represent the deformation potential energies of the reinforcement area ABCD and the deformation influence area BEFC, respectively; E_1 and E_2 represent the elastic moduli of the reinforcement area ABCD and the deformation influence area BEFC, respectively; μ_1 and μ_2 represent the Poisson's ratios of the materials in the reinforcement area ABCD and the deformation influence area BEFC, respectively.

$$\left.\begin{array}{l} \alpha_i = E_i(1-\mu_i)/((1+\mu_i)(1-2\mu_i)) \\ \beta_i = 2\mu_i/(1-\mu_i) \\ \gamma_i = (1-2\mu_i)/(2(1-\mu_i)) \end{array}\right\} (i = 1,2) \quad (8)$$

Based on Figure 1, the total deformation potential energy of the reinforcement area and the deformation influence area can be obtained using the superposition method:

$$U = U_1 + U_2 \quad (9)$$

Based on Figure 1, the potential energy of the embankment load is:

$$W_1 = -\int_{AD} Q v_m|_{y=b} dx \quad (10)$$

Based on the assumptions described earlier, the frictional resistance and the potential energy of the normal force on the AE (DF) interface are respectively:

$$W_2 = 2\int_{AE} f e_p v_m|_{x=a} dy \quad (11)$$

$$W_3 = 2\int_{AE} e_p u_m|_{x=a} dy \quad (12)$$

In the formula,f represents the coefficient of friction on the AE (DF) interface.

$$f = tg\varphi; m = 1,2,3;$$

$$u_1 = v_1 = \frac{y}{b};$$

$$u_2 = \left(\frac{\frac{x}{a-x^3}}{a^3}\right) = \frac{y}{b};$$

$$u_3 = \left(\frac{\frac{x}{a-x^3}}{a^3}\right) = \frac{y^2}{b}^2$$

$$v_2 = \frac{\left(\frac{1-x^2}{a^2}\right)y}{b;} v_3 = \frac{\left(\frac{1-x^2}{a^2}\right)y^2}{b^2}.$$

From this, the total potential energy of the system can be obtained as:

$$\Pi = U + W_1 + W_2 + W_3 \quad (13)$$

By the principle of stationary potential energy, the displacement variational equation for this problem can be derived as:

$$\sum_m [\frac{\partial U}{\partial A_m} + 2\int_{AE} e_p u_m|_{x=a} dy]\delta A_m + \sum_m [\frac{\partial U}{\partial B_m} - \int_{AD} Q v_m|_{y=b} dx + 2\int_{AE} f e_p v_m|_{x=a} dy]\delta B_m = 0 \quad (14)$$

Since the variations δA_m, δB_m (m=1,2,3) are completely arbitrary and mutually independent, their coefficients in the above equation must be equal to zero, hence we obtain:

$$\frac{\partial U}{\partial A_m} = -2\int_0^b e_p u_m|_{x=a} dy$$

$$\frac{\partial U}{\partial B_m} = 2\int_0^{L_1+L_2} Q v_m|_{y=b} dx - 2\int_0^b f e_p v_m|_{x=a} dy = 0 \quad (15)$$

By substituting Equations (1), (2), (5), (6), and (7) into Equation (15), a system of linear algebraic equations for coefficients A_m、$B_m(m = 1,2,3)$ is obtained. Solving this system of equations will yield the undetermined coefficients A_m、$B_m(m = 1,2,3)$.

From Equation (5), the settlement and horizontal displacement of points within the load-bearing range can be obtained.

3. Engineering Case Analysis

3.1 Comparison of Numerical Simulation and Theoretical Analysis Results

Taking the soft foundation treatment project of the highway at the southeast Meizhou Bay, Zhongmen Peninsula, Putian City, Fujian Province, China as an example, this paper compares the final settlement obtained using the theoretical method pro-posed herein with the stable settlement amount after 200 days of field monitoring. Additionally, the numerical simulation results were mutually verified with the theoretical analysis results and field monitoring results, confirming the feasibility and rationality of the theoretical analysis method proposed in this paper.

The soft foundation treatment project of the highway at the southeast Meizhou Bay, Zhongmen Peninsula, Putian City, Fujian Province, is shown in Figure 2. The height of the embankment fill is 7.0 m, and the unit weight of the embankment fill is 16.30 kN/m³. The geological survey report for this project indicates that there is bed-rock at a depth of 13.0 m below the original ground surface, hence the numerical simulation calculation depth is taken as 13.0 m. Within the depth range of 13.0 m, there are two soil layers: 0—10.0 m is mucky clay, and 10.0 m—13.0 m is silty clay. The depth of the cement mixing pile reinforcement is 10.0 m, with a pile diameter of 0.5 m and a pile spacing of 1.5 m. The numerical simulation calculation width is taken as 74 m, of which 24 m is the load-bearing area. The numerical simulation model takes a width of 74 m, with 24 m designated as the load-bearing area. At the edge of the load-bearing area, a soil-cement lateral retaining wall with a width of 4.0 m, formed by cement mixing piles, is set, with the wall embedded to a depth of 13.0 m. Based on the geological data of the soft foundation for this project and the actual layout of the cement

mixing piles, the calculation depth of the numerical simulation model is taken as 13 m, the width as 74 m, and the length as 1.5 m. The FLAC 3D numerical simulation model for this foundation is established as shown in Figure 2. During numerical simulation, the relevant calculation parameters for the cement mixing pile reinforcement area are determined based on the pile replacement rate, mimicking the equivalent composite modulus to establish equivalent composite parameters. The calculation parameters for each soil layer and the soil-cement wall are shown in Table 1.

Table 1: Calculation parameter of numerical simulation

Material type	Modulus of elasticity (MPa)	Poisson's ratio	Gravity (kN/m^{-3})	Cohesion (kPa)	Internal friction angle (°)
Embankment fill	7.0	0.25	20.0	0	30
Mucky soil	2.0	0.35	19.0	10.0	10
Silty clay	4.0	0.3	19.5	30.0	15
Soil-cement wall	150.0	0.3	20.0	130.0	30

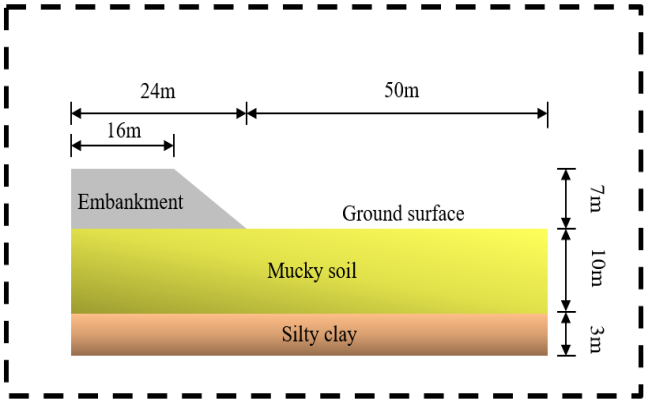

Figure 2: Model of foundation

Boundary conditions: The normal displacement is constrained in the width direction; both normal and tangential displacements are constrained at the bottom of the model; the normal displacement is constrained in the longitudinal direction of the road.

Contact surface parameters: both the normal contact stiffness k_n and the tangential contact stiffness k_s are set to 1.0×1010.

During numerical simulation, the foundation depth and road width directions are discretized with 1.0 m-sized grid cells; the road length is divided into 2 grid cells; the embankment fill uses 0.5 m-sized grid cells, totaling 2596 grid cells. The grid division for the numerical simulation is shown in Figure 3. When the width of the lateral soil-cement wall is taken as 4.0 m, the numerical simulation results are shown in Figure 4. The numerical simulation results indicate that when the width of the lateral soil-cement wall exceeds 4.0 m, the maximum settlement at the center of the embankment load remains stable at 160.3 mm. It can be concluded that when the width of the lateral soil-cement wall reaches 4.0 m, the deformation of the foundation in the load-bearing area is independent of the width of the lateral soil-cement wall. At this point, the constraint of the lateral soil-cement wall on the load-bearing area is equivalent to a rigid constraint.

The theoretical analysis results indicate that when the constraint of the lateral soil-cement wall on the load-bearing area is defined as a rigid constraint, the normal force on the AE and DF interfaces in contact with the soil is taken as the at-rest earth pressure, and the coefficient of at-rest earth pressure is taken as. By setting the undetermined coefficient A1 and B1 to 0, the maximum settlement at the center of the embankment load is found to be 146.7 mm. It can be seen that the theoretical calculation results are very close to the numerical simulation results, thereby verifying the rationality of the theoretical analysis method.

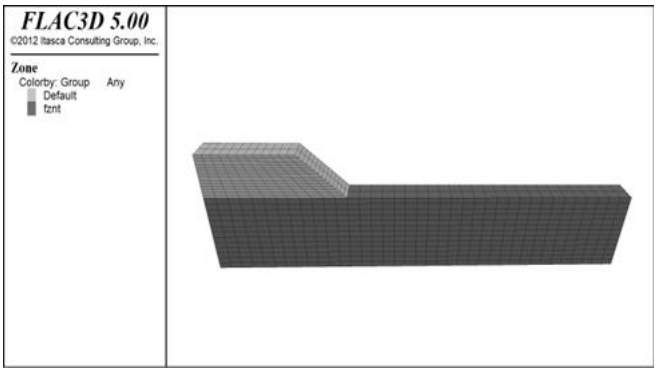

Figure 3: Mesh dividing of numerical simulation

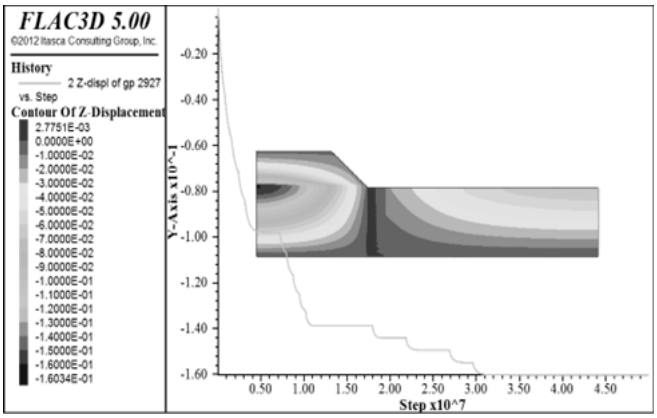

Figure 4: Results of numerical simulation.

The theoretical analysis also found that: when the normal force on the AE and DF interfaces, where the lateral soil-cement wall is in contact with the soil, is taken as the passive earth pressure, and the passive earth pressure reduction coefficient is set to 1.0, the maximum settlement at the center of the embankment load is obtained as 221.3 mm, which is close to the numerical simulation result of 261.6 mm without the lateral soil-cement wall. From the numerical simulation results, it is known that: for soft soil foundations with soil-cement lateral restriction, when the lateral restriction can completely limit the horizontal displacement of soil within the load-bearing range, the settlement at the center point of the load is reduced by nearly 40% compared to the situation without lateral restriction.

3.2 Comparison of Numerical Simulation, Theoretical Analysis, and Field Monitoring Results

The relationship between the height of embankment fill and the time of filling can be seen in Figure 5.

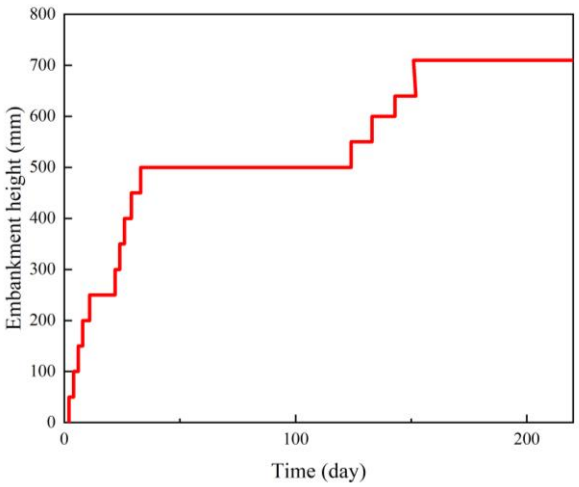

Figure 5: Relationship between embankment height and filling time

To verify the reliability of the theoretical analysis method, a field monitoring profile was selected for theoretical analysis. Figure 6 shows the comparison curve between the numerical simulation results and the field monitoring results at the center of the embankment. From Figure 6, it can be seen that at 200 days of filling time, the field monitoring results match well with the numerical simulation results. At the same time, the final settlement at the center of the embankment obtained by the theoretical analysis method proposed in this paper is 146.7 mm. At the end of the embankment filling construction, the final settlement at the center of the embankment monitored on-site was 153.6 mm. The final settlement at the center of the embankment obtained by numerical simulation was 160.3 mm. It can be seen that the results of numerical simulation, theoretical analysis, and field monitoring all match very well. This indicates the reliability and rationality of the theoretical analysis method proposed in this paper.

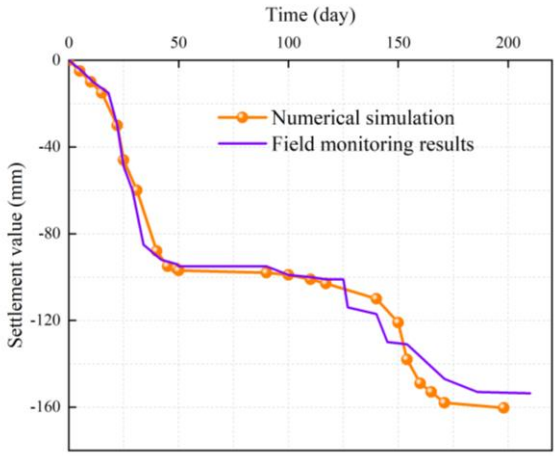

Figure 6: Comparison curve of numerical simulation and field monitoring results

4. Conclusion

This paper draws the following conclusions by comparing numerical simulation, theoretical analysis, and field monitoring results:

1) A new technology for laterally restrained flexible pile composite foundation and an energy method for deformation analysis have been proposed, which construct dis-placement component expressions that satisfy the displacement boundary conditions, establish the system's displacement variational equation, and verify the rationality of the theoretical analysis method through numerical simulation. This has good guiding significance for improving the treatment level of soft soil foundations.

2) For natural soft soil foundations or soft soil foundations reinforced with flexible piles, the use of soil-cement wall lateral restraint technology can effectively reduce the settlement of flexible pile composite foundations or soft soil foundations. The extent of settlement reduction depends on the lateral restraint stiffness of the soil-cement wall; the greater the lateral restraint stiffness, the greater the reduction in settlement.

3) If the commonly used surcharge preloading technology in soft foundation treatment methods is combined with the soil-cement wall lateral restraint technology proposed in this paper, on the one hand, it can reduce the adverse impact of surcharge preloading on the surrounding environment, as well as the ground heave and horizontal displacement of soil outside the reinforcement area; on the other hand, by set-ting the lateral restraint wall to a certain depth or having its base enter the impermeable layer, it can act as a water-stop curtain, effectively avoiding the adverse impact on the surrounding environment due to the lowering of the groundwater level in the reinforcement area. At the same time, it can effectively shorten the surcharge preloading time and improve the effect of surcharge preloading. The influence of lateral restraint on surcharge preloading will be discussed in another paper.

Acknowledgments

This research is financially supported by the National Natural Science Foundation of China (51978260).

References

[1] Wang F, Jin W, Wang H K. Amendment of subgrade settlement of passenger dedicated line considering the lateral deformation effects[J]. Chinese Journal of Geotechnical Engineering, 2010, 32(Sup 2): 245-248.

[2] Alamgir M, Miura N, Poorooshasb H B, et al. Deformation analysis of soft ground reinforced by columnar inclusions[J]. Computers and Geotechnics, 1996, 18(4): 267-290.

[3] Loganathan N, Balasubramaniam A S, Bergado D T. Deformation analysis of embankments[J]. Journal of Geotechnical Engineering, 1993, 119(8): 1185-1206.

[4] Tu Y, Zheng J. Analysis of embankment settlement considering soil lateral dilation behavior[J]. China Journal of Highway and Transport, 2002, 15(1): 26-28.

[5] Zhi-liang W, Yong-chi L I, Zong-ze Y I N. Discussion on settlement calculation of embankment considering lateral dilation behavior of soils[J]. Chinese Journal of Rock Mechanics and Engineering, 2005, 24(10): 1772-1777.

[6] Wen-zhi L, Jian-lin Y, Xiao-nan G. Parameter analysis of pile foundation under flexible foundation [J]. Journal of Rock Mechanics and Engineering, 2010, 29 (2): 401-408.

[7] Wu Y, Fu L, Wu W, et al. Nonlinear stress analysis of flexible pile composite foundation by energy method[J]. Advances in Materials Science and Engineering, 2018, 2018(1): 8176398.
[8] Lv W, Yu J, Gong X. Analytical method for pile composite ground under flexible foundation[J]. Chinese Journal of Rock Mechanics and Engineering, 2010, 29(2): 401-408.
[9] Song H L, Zhao R F, Zhao G T. Calculation method for composite modulus of flexible pile composite foundation for high-speed railway under post-work settlement source[J]. Construction and Building Materials, 2024, 411: 134576.
[10] Ye G, Cai Y, Zhang Z. Numerical study on load transfer effect of Stiffened Deep Mixed column-supported embankment over soft soil. KSCE J Civ Eng 21: 703–714[EB/OL].(2017)
[11] Jenck O, Dias D, Kastner R. Discrete element modelling of a granular platform supported by piles in soft soil–Validation on a small scale model test and comparison to a numerical analysis in a continuum[J]. Computers and Geotechnics, 2009, 36(6): 917-927
[12] Gourvenec S, Acosta-Martinez H E, Randolph M F. Experimental study of uplift resistance of shallow skirted foundations in clay under transient and sustained concentric loading[J]. Géotechnique, 2009, 59(6): 525-537
[13] Dong Y, Feng Z, He J, et al. An analytical solution for the load-settlement relation of hollow composite piles with ultra-large diameters[J]. Physics and Chemistry of the Earth, Parts A/B/C, 2023, 132: 103466.
[14] Ishikura R, Yasufuku N, Brown M J. An estimation method for predicting final consolidation settlement of ground improved by floating soil cement columns[J]. Soils and Foundations, 2016, 56(2): 213-227.
[15] Zhao M, Liu M, Ma B, et al. Calculation of pile-soil stress ratio and settlement of pile-net composite foundation based on elastic foundation plate[J]. Journal of Central South University, 2016, 47(6): 2007-2014.
[16] Ma Q, Mou J, Xiao H. Experimental and numerical studies on bearing characteristics of hexagonal-section composite foundation element[J]. Iranian Journal of Science and Technology, Transactions of Civil Engineering, 2021, 45: 929-939.
[17] Qing-zi L, Xiao-ping C. Deformation behavior and consolidation model of soft soil under flexible lateral constraint [J]. Rock and Soil Mechanics, 2019, 40(06): 2264-2274.
[18] Yu J, Chen J, Zhou J, et al. Analytical modeling for the behavior of concrete-cored cement mixing (CCM) pile composite foundation under embankment[J]. Computers and Geotechnics, 2024, 167: 106084.
[19] Alamgir M, Miura N, Poorooshasb H B, et al. Deformation analysis of soft ground reinforced by columnar inclusions[J]. Computers and Geotechnics, 1996, 18(4): 267-290.
[20] Yu J, Zhou J, Gong X, et al. Centrifuge study on behavior of rigid pile composite foundation under embankment in soft soil[J]. Acta Geotechnica, 2021, 16: 1909-1921.
[21] Phutthananon C, Jongpradist P, Wonglert A, et al. Field and 3D numerical investigations of the performances of stiffened deep cement mixing column-supported embankments built on soft soil[J]. Arabian Journal for Science and Engineering, 2023, 48(4): 5139-5169.
[22] Zhang M, Zhu H, Chen L, et al. Experimental Study for the Geogrid-Reinforced Embankment with Clay Cover Under Static and Cyclic Loading[J]. International Journal of Civil Engineering, 2024, 22(2): 181-194.
[23] Bathurst R J, Vlachopoulos N, Walters D L, et al. The influence of facing stiffness on the performance of two geosynthetic reinforced soil retaining walls[J]. Canadian Geotechnical Journal, 2006, 43(12): 1225-1237.
[24] Miao L, Wang F, Lv W. A simplified calculation method for stress concentration ratio of composite foundation with rigid piles[J]. KSCE Journal of Civil Engineering, 2018, 22: 3263-3270.
[25] Cao F, Ye C, Wu Z, et al. Settlement Calculation of Semi-Rigid Pile Composite Foundation on Ultra-Soft Soil under Embankment Load[J]. Buildings, 2024, 14(7): 1954.
[26] Madhira M, Kiran K V. A Method to Estimate Shaft and Base Responses of a Pile from Pile Load Test Results[J]. Geotechnical Engineering (00465828), 2019, 50(3).
[27] Wu C, Yu J, Cao X, et al. Study on Design Method of Pile Wall Combination Structure in a Deep Foundation Pit Considering Deformation Induced by Excavation[J]. Frontiers in Earth Science, 2022, 10: 837950.
[28] Ministry of Transport of the People's Republic of China. Specifications for Design of Highway Subgrades (JTG D30-2015) [S]. Beijing: China Communications Press, 2015. (In Chinese).